

Learning Model Reparametrizations: Implicit Variational Inference by Fitting MCMC distributions

Michalis K. Titsias

Department of Informatics,
Athens University of Economics and Business,
Athens, Greece

August 7, 2017

Abstract

We introduce a new algorithm for approximate inference that combines reparametrization, Markov chain Monte Carlo and variational methods. We construct a very flexible implicit variational distribution synthesized by an arbitrary Markov chain Monte Carlo operation and a deterministic transformation that can be optimized using the reparametrization trick. Unlike current methods for implicit variational inference, our method avoids the computation of log density ratios and therefore it is easily applicable to arbitrary continuous and differentiable models. We demonstrate the proposed algorithm for fitting banana-shaped distributions and for training variational autoencoders.

1 Introduction

Consider a probabilistic model with joint distribution $p(\mathbf{x}, \mathbf{z})$ where \mathbf{x} are data and \mathbf{z} are latent variables and/or random parameters. Suppose that exact inference in $p(\mathbf{x}, \mathbf{z})$ is intractable which means that the posterior distribution

$$p(\mathbf{z}|\mathbf{x}) = \frac{p(\mathbf{x}, \mathbf{z})}{\int p(\mathbf{x}, \mathbf{z})d\mathbf{z}},$$

is difficult to compute due to the normalizing constant $p(\mathbf{x}) = \int p(\mathbf{x}, \mathbf{z})d\mathbf{z}$ that represents the probability of the data and it is known as evidence or marginal likelihood. The marginal likelihood is essential for estimation of any extra parameters in $p(\mathbf{x})$ or for model comparison. Approximate inference algorithms target to approximate $p(\mathbf{z}|\mathbf{x})$ and/or $p(\mathbf{x})$. Two general frameworks, that we briefly review next, are based on Markov chain Monte Carlo (MCMC) [33, 2] and variational inference (VI) [17, 40].

MCMC constructs a Markov chain with transition kernel $q(\mathbf{z}'|\mathbf{z})$ that leaves $p(\mathbf{z}|\mathbf{x})$ invariant, i.e.

$$p(\mathbf{z}'|\mathbf{x}) = \int q(\mathbf{z}'|\mathbf{z})p(\mathbf{z}|\mathbf{x})d\mathbf{z}.$$

There exist many popular MCMC algorithms, such as random walk Metropolis-Hastings, Gibbs sampling, Metropolis-adjusted Langevin and Hamiltonian Monte Carlo; for detailed discussions see [33, 2]. The great advantage of MCMC is that it offers a very flexible non-parametric inference procedure that is exact in the limit of long/infinite runs. The main disadvantage of MCMC is that it may require a long time to converge, i.e. for the corresponding chain to

produce an independent sample from $p(\mathbf{z}|\mathbf{x})$. Even after convergence the produced samples are statistically dependent and can exhibit high autocorrelation. Advances on adaptive MCMC [12, 1], Hamiltonian Monte Carlo [8, 25, 15] and Riemann manifold methods [9] try to speed up MCMC convergence and improve on statistical efficiency, but the general problem is still far from been solved.

In contrast, VI carries out approximate inference by fitting parametric distributions to the exact distributions using optimization. To approximate the exact posterior $p(\mathbf{z}|\mathbf{x})$ a distribution $q(\mathbf{z}; \boldsymbol{\theta})$ is introduced, that belongs to a tractable variational family, and the parameters $\boldsymbol{\theta}$ are fitted by minimizing a distance measure between the two distributions. The most widely used VI algorithms are based on minimizing the KL divergence between $q(\mathbf{z}; \boldsymbol{\theta})$ and $p(\mathbf{z}|\mathbf{x})$ so that

$$\boldsymbol{\theta}^* = \arg \min_{\boldsymbol{\theta}} \text{KL}(q(\mathbf{z}; \boldsymbol{\theta}) || p(\mathbf{z}|\mathbf{x})).$$

This minimization can be equivalently expressed as a maximization of a lower bound on the log marginal likelihood,

$$\mathcal{F}(\boldsymbol{\theta}) = \mathbb{E}_{q(\mathbf{z}; \boldsymbol{\theta})}[\log p(\mathbf{x}, \mathbf{z}) - \log q(\mathbf{z}; \boldsymbol{\theta})] \leq \log p(\mathbf{x}). \quad (1)$$

An advantage of VI is that turns approximate inference into optimization which typically results in much faster algorithms than MCMC methods. The disadvantage, however, is that in order for the optimization procedure to be fast or tractable the parametric distribution $q(\mathbf{z}; \boldsymbol{\theta})$ needs to be oversimplified which often leads to poor approximations. An influential recent technique used in VI is stochastic optimization [32] that allows to extend traditional VI algorithms to big data [13, 14] and to nonconjugate probabilistic models [3, 26, 28, 24, 38, 35, 19, 30]. Indeed, by using stochastic optimization VI has become a fully general inference method applicable to arbitrary probabilistic models, as those expressible by probabilistic programming languages such as Stan [4, 20]. Stochastic optimization has also opened new directions towards increasing the flexibility of the parametric variational family by using normalizing flows [31] or by allowing $q(\mathbf{z}; \boldsymbol{\theta})$ to be an implicit distribution [29, 22, 41, 18, 23, 16, 39]. However, the increased flexibility of the parametric distribution $q(\mathbf{z}; \boldsymbol{\theta})$ often results in slow and less stable optimization. For instance, recent implicit variational methods [18, 23, 16, 39] that utilise arbitrarily flexible parametric families for $q(\mathbf{z}; \boldsymbol{\theta})$ require the computation of log density ratios [37], which is a very difficult problem in high dimensional settings. This implies that there is a (rather obvious) trade off between optimization efficiency and complexity of the parametric variational family; the more parameters and non-linear structure $q(\mathbf{z}; \boldsymbol{\theta})$ has, the more difficult the optimization becomes.

In this paper we propose to increase the flexibility of the variational family, and thus the approximation capacity of the inference procedure, not by adding more parameters and non-linearities but instead through the synthesis of MCMC and a model-based learnable reparametrization. On one hand, MCMC will allow us to increase the flexibility of the variational family by making it non-parametric and on the other hand the learnable reparametrization will allow us to optimize the MCMC-based variational family by tuning a small set of parameters, such as parameters that define an affine transformation. This yields a MCMC-based implicit variational approximation that can be optimized using a procedure that, in terms of stability, behaves similarly to the standard reparametrization-based stochastic VI algorithms that fit Gaussian approximations [38, 19, 30]. Furthermore, unlike other implicit variational inference methods [18, 23, 16, 39], the proposed algorithm does not require the computation of log density ratios.

The remainder of this paper has as follows. Section 2 develops the theory of the proposed method. Section 3 discusses related work such as the recent work in [21] that learns how to distil MCMC. Section 4 presents experiments on fitting banana-shaped distributions and for training variational autoencoders, while Section 5 concludes with a discussion.

2 Combine variational inference, MCMC and reparametrization

Section 2.1 discusses a key concept of our method that is related to learnable model-based reparametrizations. Then Section 2.2 introduces the algorithm that combines reparametrization, MCMC and variational inference.

2.1 Model-based reparametrizations

The reparametrization trick plays a prominent role in modern approximate inference methods. The currently popular view of this trick is *approximation-based* where the reparametrization is assumed to be a characteristic of a variational family of distributions $\{q(\mathbf{z}; \boldsymbol{\theta}), \forall \boldsymbol{\theta} \in \Theta\}$ so that a sample $\mathbf{z} \sim q(\mathbf{z}; \boldsymbol{\theta})$ can be constructed by first drawing a latent noise variable $\boldsymbol{\epsilon} \sim p(\boldsymbol{\epsilon})$ and then applying a transformation $\mathbf{z} = g(\boldsymbol{\epsilon}; \boldsymbol{\theta})$. Whether the distribution $q(\mathbf{z}; \boldsymbol{\theta})$ will be known explicitly or implicitly (i.e. its density will be analytic or not) depends on the properties of both the noise distribution $p(\boldsymbol{\epsilon})$ and the mapping $g(\boldsymbol{\epsilon}; \boldsymbol{\theta})$. Approximate inference then proceeds by fitting $q(\mathbf{z}; \boldsymbol{\theta})$ to the exact posterior distribution. This is typically based on the standard procedure that minimizes the KL divergence $\text{KL}(q(\mathbf{z}; \boldsymbol{\theta}) || p(\mathbf{z} | \mathbf{x}))$. The ability to reparametrize $q(\mathbf{z}; \boldsymbol{\theta})$ allows us to speed up the stochastic optimization of the variational parameters $\boldsymbol{\theta}$ by making use of gradients of the log model density $\log p(\mathbf{x}, \mathbf{z})$ [38, 19, 30, 34]. To summarize in the approximation-based view of reparametrization we leave the model $p(\mathbf{x}, \mathbf{z})$ unchanged and we reparametrize some variational approximation to this model.

An alternative way to apply reparametrization is *model-based*. Here, we reparametrize directly the model $p(\mathbf{x}, \mathbf{z})$ in order to obtain a new model representation and then we apply (approximate) inference in this new representation. The inference procedure could be based on any framework such as exact inference (if possible), MCMC or variational methods. The objectives of model-based reparametrizations are similar with the ones of approximation-based reparametrizations, i.e. we would like to make inference and parameter estimation as easy as possible. Several examples of model-based reparametrizations have been used in the literature, such as the centered and non-centered reparametrizations [27]. These reparametrizations are typically model-specific and they are not learnable during inference. Next we develop a generic methodology for continuous spaces and in Section 2.2 we develop an algorithm that automatically can learn model-based reparametrizations.

A valid reparametrization of $p(\mathbf{x}, \mathbf{z})$ essentially performs a transformation of \mathbf{z} into a new set of random variables $\boldsymbol{\epsilon}$ so that the probability of the observed data $p(\mathbf{x})$ remains unchanged, i.e. we have the following marginal likelihood invariance property

$$p(\mathbf{x}) = \int p(\mathbf{x}, \mathbf{z}) d\mathbf{z} = \int p(\mathbf{x}, \boldsymbol{\epsilon}) d\boldsymbol{\epsilon}.$$

Given that \mathbf{z} is continuous and $p(\mathbf{x}, \mathbf{z})$ is differentiable w.r.t. \mathbf{z} a generic way to define a valid reparametrization is through an invertible transformation

$$\boldsymbol{\epsilon} = g^{-1}(\mathbf{z}; \boldsymbol{\theta}), \quad \mathbf{z} = g(\boldsymbol{\epsilon}; \boldsymbol{\theta}).$$

Then the reparametrized model becomes

$$p(\mathbf{x}, \boldsymbol{\epsilon}; \boldsymbol{\theta}) = p(\mathbf{x}, g(\boldsymbol{\epsilon}; \boldsymbol{\theta})) J(\boldsymbol{\epsilon}; \boldsymbol{\theta}), \tag{2}$$

where $J(\boldsymbol{\epsilon}; \boldsymbol{\theta}) = |\det \nabla_{\boldsymbol{\epsilon}} g(\boldsymbol{\epsilon}; \boldsymbol{\theta})|$ denotes the determinant of the Jacobian of the transformation. The marginal likelihood is

$$p(\mathbf{x}) = \int p(\mathbf{x}, g(\boldsymbol{\epsilon}; \boldsymbol{\theta})) J(\boldsymbol{\epsilon}; \boldsymbol{\theta}) d\boldsymbol{\epsilon},$$

which clearly is equal to the marginal likelihood $\int p(\mathbf{x}, \mathbf{z}) d\mathbf{z}$ computed from the initial representation. Thus, a first noticeable property of the reparametrized model is that while $\boldsymbol{\theta}$ enters the expression in (2) superficially as a *new model parameter*, it does not change the value of the marginal probability $p(\mathbf{x})$. Therefore, $\boldsymbol{\theta}$ is not a model parameter that can influence the fit to the observed data \mathbf{x} . In contrast the reparametrized posterior distribution $p(\boldsymbol{\epsilon}|\mathbf{x}, \boldsymbol{\theta}) \propto p(\mathbf{x}, g(\boldsymbol{\epsilon}; \boldsymbol{\theta}))J(\boldsymbol{\epsilon}; \boldsymbol{\theta})$ does depend on $\boldsymbol{\theta}$, although notice that by transforming an exact sample from $p(\boldsymbol{\epsilon}|\mathbf{x}, \boldsymbol{\theta})$ back to the space of \mathbf{z} we always get an exact sample from $p(\mathbf{z}|\mathbf{x})$ irrespectively of the value of $\boldsymbol{\theta}$. It is precisely this dependence of $p(\boldsymbol{\epsilon}|\mathbf{x}, \boldsymbol{\theta})$ on $\boldsymbol{\theta}$ that we would like to exploit in order to improve the accuracy and/or computational efficiency of approximate inference methods. For instance, if $g(\boldsymbol{\epsilon}; \boldsymbol{\theta})$ is chosen so that $p(\boldsymbol{\epsilon}|\mathbf{x}, \boldsymbol{\theta})$ becomes roughly independent across the dimensions of $\boldsymbol{\epsilon}$, then simple inference methods such mean field variational approximations or Gibbs sampling will be very effective.¹

Next we introduce a variational inference and MCMC hybrid algorithm that directly operates in the reparametrized model and it can auto-tune its performance by optimizing $\boldsymbol{\theta}$.

2.2 Implicit MCMC-based variational inference

Assume an arbitrary MCMC algorithm, such as standard random walk Metropolis-Hastings or more advanced schemes like Hamiltonian Monte Carlo that is very popular in probabilistic programming systems [4], having a transition kernel $q(\boldsymbol{\epsilon}'|\boldsymbol{\epsilon})$ that leaves the posterior distribution $p(\boldsymbol{\epsilon}|\mathbf{x}, \boldsymbol{\theta})$ invariant, i.e.

$$p(\boldsymbol{\epsilon}'|\mathbf{x}, \boldsymbol{\theta}) = \int q(\boldsymbol{\epsilon}'|\boldsymbol{\epsilon})p(\boldsymbol{\epsilon}|\mathbf{x}, \boldsymbol{\theta})d\boldsymbol{\epsilon}.$$

Given some specific value for $\boldsymbol{\theta}$, if we apply the MCMC algorithm for long enough we will eventually converge to the posterior distribution. This translates to convergence to the initial posterior distribution $p(\mathbf{z}|\mathbf{x})$ irrespectively of the chosen value $\boldsymbol{\theta}$. This somehow gives us the freedom to adapt $\boldsymbol{\theta}$ so that to speed up convergence to $p(\boldsymbol{\epsilon}|\mathbf{x}, \boldsymbol{\theta})$ and essentially to $p(\mathbf{z}|\mathbf{x})$. So we need a learning procedure to tune $\boldsymbol{\theta}$ and next we shall use variational inference. Specifically, we assume that MCMC is initialized with some fixed distribution $q_0(\boldsymbol{\epsilon})$ and then the transition kernel is applied for a fixed number of t iterations. This constructs the marginal MCMC distribution

$$q_t(\boldsymbol{\epsilon}) = \int Q_t(\boldsymbol{\epsilon}|\boldsymbol{\epsilon}_0)q_0(\boldsymbol{\epsilon}_0)d\boldsymbol{\epsilon}_0,$$

where $Q_t(\boldsymbol{\epsilon}'|\boldsymbol{\epsilon}_0)$ is the compound transition density obtained by applying t times the transition kernel $q(\boldsymbol{\epsilon}'|\boldsymbol{\epsilon})$. $q_t(\boldsymbol{\epsilon})$ is an implicit distribution since we can only draw samples from it but we cannot evaluate $q_t(\boldsymbol{\epsilon})$. Nevertheless, by following the recent advances in implicit variational inference [18, 23, 16, 39] we shall consider $q_t(\boldsymbol{\epsilon})$ as the variational distribution and fit it to the exact posterior $p(\boldsymbol{\epsilon}|\mathbf{x}, \boldsymbol{\theta})$ by minimizing the KL divergence $\text{KL}(q_t(\boldsymbol{\epsilon})||p(\boldsymbol{\epsilon}|\mathbf{x}, \boldsymbol{\theta}))$ which leads to the maximization of the standard lower bound

$$\mathcal{F}_t(\boldsymbol{\theta}) = \int q_t(\boldsymbol{\epsilon}) [\log p(\mathbf{x}, g(\boldsymbol{\epsilon}; \boldsymbol{\theta}))J(\boldsymbol{\epsilon}; \boldsymbol{\theta}) - \log q_t(\boldsymbol{\epsilon})] d\boldsymbol{\epsilon}. \quad (3)$$

Unlike the exact marginal likelihood, this bound does depend on the parameters $\boldsymbol{\theta}$ which now become variational parameters that can be tuned to improve the approximation. Also notice that, unlike the standard way of thinking about variational lower bounds where the variational parameters are defined to directly influence the variational distribution, in the above bound the

¹The mean field approximation will capture accurately the dependence structure of the posterior, while Gibbs sampling will enjoy high statistical efficiency producing essentially an independent sample in every iteration.

variational parameters $\boldsymbol{\theta}$ are essentially part of the log joint density and rather indirectly influence $q_t(\boldsymbol{\epsilon})$. Thus, when we maximize $\mathcal{F}_t(\boldsymbol{\theta})$ we essentially try to transform the reparametrized exact posterior distribution $p(\boldsymbol{\epsilon}|\mathbf{x}, \boldsymbol{\theta})$ so that to make it more easily reachable by the MCMC marginal $q_t(\boldsymbol{\epsilon})$. We can express the equivalent standard view of the variational lower bound in (3) by changing variables and re-writing $\mathcal{F}_t(\boldsymbol{\theta})$ as

$$\mathcal{F}_t(\boldsymbol{\theta}) = \int q_t(\mathbf{z}; \boldsymbol{\theta}) [\log p(\mathbf{x}, \mathbf{z}) - \log q_t(\mathbf{z}; \boldsymbol{\theta})] d\mathbf{z},$$

where

$$q_t(\mathbf{z}; \boldsymbol{\theta}) = q_t(g^{-1}(\mathbf{z}; \boldsymbol{\theta})) \tilde{J}(\mathbf{z}; \boldsymbol{\theta})$$

and $\tilde{J}(\mathbf{z}; \boldsymbol{\theta}) = |\det \nabla_{\mathbf{z}} g^{-1}(\mathbf{z}; \boldsymbol{\theta})|$ denotes the determinant of the Jacobian associated with the inverse transformation $g^{-1}(\mathbf{z}; \boldsymbol{\theta})$. This clearly shows that the induced variational distribution $q_t(\mathbf{z}; \boldsymbol{\theta})$ is reparametrizable and is made up by an implicit MCMC marginal $q_t(\boldsymbol{\epsilon})$, that operates in the space of $\boldsymbol{\epsilon}$, followed by an invertible transformation that maps $\boldsymbol{\epsilon}$ to \mathbf{z} .

To maximize (3) w.r.t. $\boldsymbol{\theta}$ we can use an algorithm similar to Monte Carlo EM [42]. Suppose we are at the k -th iteration of the optimization, where the previous value of the parameter vector is $\boldsymbol{\theta}_{k-1}$. We first perform an E-step where MCMC dynamics flow through the unnormalized posterior $p(\mathbf{x}, g(\boldsymbol{\epsilon}; \boldsymbol{\theta}_{k-1}))J(\boldsymbol{\epsilon}; \boldsymbol{\theta}_{k-1})$ for t iterations which produces an independent sample from $q_t(\boldsymbol{\epsilon})$. By repeating this process S times we can produce a set of S independent samples $\{\boldsymbol{\epsilon}^{(s)}\}_{s=1}^S$. Then we perform an M-step where we keep the approximate posterior $q_t(\boldsymbol{\epsilon})$ fixed and we maximize the following Monte Carlo approximation of (3) with respect to $\boldsymbol{\theta}$

$$\frac{1}{S} \sum_{s=1}^S \log p(\mathbf{x}, g(\boldsymbol{\epsilon}^{(s)}; \boldsymbol{\theta}))J(\boldsymbol{\epsilon}^{(s)}; \boldsymbol{\theta}),$$

where the constant entropic term $-\int q_t(\boldsymbol{\epsilon}) \log q_t(\boldsymbol{\epsilon}) d\boldsymbol{\epsilon}$ has been dropped since it does not depend on $\boldsymbol{\theta}$ ($q_t(\boldsymbol{\epsilon})$ depends on the old values $\boldsymbol{\theta}_{k-1}$). We can take a step towards maximizing this Monte Carlo objective by performing a gradient ascent step,

$$\boldsymbol{\theta}_k = \boldsymbol{\theta}_{k-1} + \eta_k \frac{1}{S} \sum_{s=1}^S \nabla_{\boldsymbol{\theta}=\boldsymbol{\theta}_{k-1}} \log p(\mathbf{x}, g(\boldsymbol{\epsilon}^{(s)}; \boldsymbol{\theta}))J(\boldsymbol{\epsilon}^{(s)}; \boldsymbol{\theta}),$$

where η_k denotes the learning rate. Algorithm 1 shows all steps of the procedure where for simplicity we have assumed that $S = 1$ and we have added another update for any possible model parameters \mathbf{w} that determine the joint probability density and for which we do point estimation.

To implement the algorithm the user needs to specify: i) the invertible transformation $g(\boldsymbol{\epsilon}; \boldsymbol{\theta})$, ii) the initial MCMC distribution $q_0(\boldsymbol{\epsilon})$ and iii) the MCMC kernel density together with the number of iterations t that overall define the implicit density $Q_t(\boldsymbol{\epsilon}'|\boldsymbol{\epsilon}_0)$. By varying the above options we are truly blending between variational inference and MCMC and for instance we can easily recognise the following extremes cases:

1. When $t = 0$ (i.e. there is no MCMC and $q_t(\boldsymbol{\epsilon})$ collapses to $q_0(\boldsymbol{\epsilon})$), $g(\boldsymbol{\epsilon}; \boldsymbol{\theta}) = L\boldsymbol{\epsilon} + \boldsymbol{\mu}$ and $q_0(\boldsymbol{\epsilon}) = \mathcal{N}(\boldsymbol{\epsilon}|\mathbf{0}, I)$ the method becomes the standard reparametrization-based variational inference algorithm that fits a Gaussian approximation to the true posterior [38, 5].
2. When $t = 0$, $g(\boldsymbol{\epsilon}; \boldsymbol{\theta}) = \boldsymbol{\epsilon} + \boldsymbol{\mu}$ and $q_0(\boldsymbol{\epsilon}) = \delta(\boldsymbol{\epsilon})$ the method leads to maximum a posteriori estimation.

Algorithm 1 Implicit MCMC-based variational inference using reparametrization

```
Initialize  $\boldsymbol{\theta}_0, \mathbf{w}_0, k = 0$ 
repeat
  k = k+1
  Update reparametrization parameters:
    % initialize MCMC:
     $\boldsymbol{\epsilon}_0 \sim q_0(\boldsymbol{\epsilon}_0)$ ,
    % MCMC for  $t$  iterations targeting the unnormalized  $p(\mathbf{x}, g(\boldsymbol{\epsilon}; \boldsymbol{\theta}_{k-1}))J(\boldsymbol{\epsilon}; \boldsymbol{\theta}_{k-1})$ :
     $\boldsymbol{\epsilon} \sim Q_t(\boldsymbol{\epsilon}|\boldsymbol{\epsilon}_0)$ ,
     $\boldsymbol{\theta}_k = \boldsymbol{\theta}_{k-1} + \eta_k \nabla_{\boldsymbol{\theta}=\boldsymbol{\theta}_{k-1}} \log p(\mathbf{x}, g(\boldsymbol{\epsilon}; \boldsymbol{\theta}))J(\boldsymbol{\epsilon}; \boldsymbol{\theta})$ ,
  Update model parameters:
     $\boldsymbol{\epsilon}_0 \sim q_0(\boldsymbol{\epsilon}_0)$ ,
    % MCMC for  $t$  iterations targeting the unnormalized  $p(\mathbf{x}, g(\boldsymbol{\epsilon}; \boldsymbol{\theta}_k))J(\boldsymbol{\epsilon}; \boldsymbol{\theta}_k)$ :
     $\boldsymbol{\epsilon} \sim Q_t(\boldsymbol{\epsilon}|\boldsymbol{\epsilon}_0)$ ,
     $\mathbf{z} = g(\boldsymbol{\epsilon}; \boldsymbol{\theta}_k)$ ,
     $\mathbf{w}_k = \mathbf{w}_{k-1} + \rho_k \nabla_{\mathbf{w}=\mathbf{w}_{k-1}} \log p(\mathbf{x}, \mathbf{z})$ ,
until convergence criterion is met.
```

3. When $g(\boldsymbol{\epsilon}; \boldsymbol{\theta}) = \boldsymbol{\epsilon}$ and we consider large t , the method reduces to standard Monte Carlo EM or standard MCMC (in case there are no model parameters \mathbf{w} for which we do point estimation).

Furthermore, according to the well-known inequality $\text{KL}(q_t(\boldsymbol{\epsilon})||p(\boldsymbol{\epsilon}|\mathbf{x}, \boldsymbol{\theta})) \leq \text{KL}(q_{t-1}(\boldsymbol{\epsilon})||p(\boldsymbol{\epsilon}|\mathbf{x}, \boldsymbol{\theta}))$ [6] the approximation monotonically improves as we increase the number t of MCMC iterations. Specifically, from this inequality and the fact that the MCMC marginal $q_t(\boldsymbol{\epsilon})$ converges to $p(\boldsymbol{\epsilon}|\mathbf{x}, \boldsymbol{\theta})$ as t increases we can conclude that the lower bound in (3) satisfies

$$\mathcal{F}_t(\boldsymbol{\theta}) \geq \mathcal{F}_{t-1}(\boldsymbol{\theta}), \quad \mathcal{F}_\infty(\boldsymbol{\theta}) = \log p(\mathbf{x}).$$

While this monotonic improvement with the iterations holds also for the regular MCMC, the promise of our approach is that by learning the reparametrization parameters $\boldsymbol{\theta}$ we can obtain efficient approximations even with small t . An illustrative example of this will be given in Section 4.1 using a banana-shaped distribution.

3 Related work

The proposed algorithm performs approximate inference by fitting an implicit distribution and therefore it shares similarities with other implicit variational inference methods such as [29, 22, 41, 18, 23, 16, 39]. Such approaches construct an implicit distribution by considering a tractable noise distribution $q(\boldsymbol{\epsilon})$ and then passing $\boldsymbol{\epsilon}$ through a complex non-invertible neural network mapping $\mathbf{z} = f(\boldsymbol{\epsilon}; \boldsymbol{\theta})$. In contrast, our method does the opposite, i.e. it considers an implicit complex noise distribution $q_t(\boldsymbol{\epsilon})$ (obtained by MCMC) and it passes $\boldsymbol{\epsilon}$ through a simple (invertible) transformation $\mathbf{z} = g(\boldsymbol{\epsilon}; \boldsymbol{\theta})$. This avoids the need for computing density ratios which is a significant computational advantage of our approach relative to other implicit variational inference methods. Furthermore, our method can be viewed as an extension of the standard reparametrization-based stochastic VI algorithms that fit Gaussian approximations [38, 19, 30]. Specifically, [38] considers a reparametrization-based variational approximation having two separate components that the user can specify independently: the so-called neutral or noise distribution and a deterministic transformation. Here, we allowed the neutral distribution

in [38] to become an implicit MCMC distribution, while before it had a simple parametric form such as Gaussian or uniform.

Regarding other MCMC and VI hybrid algorithms our method is closely related to the recent work in [21] which is based on learning how to distil MCMC. Our method differs since it directly maximizes a single cost function which is the standard lower bound, while in [21] there is an additional cost function that tries to project $q(\mathbf{z}; \boldsymbol{\theta})$ to the MCMC distribution. The use of two cost functions could cause convergence problems. Notice, however, that the approach in [21] is fully general while our method is applicable only to continuous and differentiable probabilistic models. A more distantly related method is the work in [36] which combines MCMC and variational inference by introducing several auxiliary variables (associated with the MCMC iterations) and corresponding auxiliary models that need to be fitted. Our method instead directly fits an MCMC distribution to the exact posterior distribution without requiring the augmentation with auxiliary variables and learning auxiliary models. Finally, another more distantly related method that interpolates between Langevin dynamics [43] and reparametrization-based stochastic VI was introduced in [7].

4 Experiments

Section 4.1 considers a banana-shaped distribution, while Section 4.2 applies the proposed method to amortised inference and variational autoencoders.

4.1 Fitting a banana-shaped distribution

As an illustrative example we consider the banana-shaped distribution often used to demonstrate adaptive MCMC methods [12]. This is defined by taking a two-dimensional Gaussian distribution with unit variances and covariance ρ and transform it so that the Gaussian coordinates $(\tilde{z}_1, \tilde{z}_2)$ become

$$z_1 = \alpha \tilde{z}_1, \quad z_2 = \frac{\tilde{z}_2}{\alpha} - b(z_1^2 + \alpha).$$

We set $\rho = 0.9$ and $\alpha = \beta = 1$ which defines the distribution with contours shown in Figure 1(a) and exact samples shown in Figure 1(b). We first apply MCMC using a random walk Metropolis-Hastings Gaussian proposal $q(\mathbf{z}'|\mathbf{z}) = \mathcal{N}(\mathbf{z}'|\mathbf{z}, \delta I)$ where the step size δ was set to $\delta = 0.5$ that leads to acceptance rates above 40%. The initial distribution was set to $q_0(\mathbf{z}_0) = \mathcal{N}(\mathbf{z}_0|\boldsymbol{\mu}_0, I)$, with $\boldsymbol{\mu}_0 = [0 \ -12]^T$, depicted by the green contours in Figure 2. We investigate several marginal MCMC distributions $q_t(\mathbf{z})$ for different values $t = 5, 20, 250, 100, 500, 1000$. Figure 2 shows independent samples from all these marginals where we can observe that MCMC converges slowly and even after 1000 iterations we don't get an independent sample from the target. Convergence in this example requires few thousands of iterations. Notice that the way we apply MCMC in this example is rather unusual since we restart the chain every t iterations in order to produce independent samples from a certain marginal $q_t(\mathbf{z})$. An advantage of this is that different runs of the chain are trivially parallelizable and when for a certain t we have converged all produced samples are truly independent samples from the target. On the other hand, the usual way to run MCMC is based on a single non-parallelizable long chain that even when convergence occurs subsequent samples are dependent and could exhibit high autocorrelation. Also as mentioned in Section 2.2 the whole procedure is a special case of Algorithm 1 where $g(\boldsymbol{\epsilon}, \boldsymbol{\theta})$ is chosen to be the identity transformation, i.e. $\mathbf{z} = g(\boldsymbol{\epsilon}, \boldsymbol{\theta}) = \boldsymbol{\epsilon}$. Next we show that by choosing a different transformation having tunable parameters we can significantly improve the approximate inference procedure. We consider the affine transformation

$$\mathbf{z} = L\boldsymbol{\epsilon} + \boldsymbol{\mu},$$

where L is lower triangular positive definite matrix and $\boldsymbol{\mu}$ a mean vector. This transformation is the standard one used in the generic reparametrization-based stochastic VI [38, 19, 30] and it can be easily extended to account for constraints in the range of values of \mathbf{z} as done in Stan [20]. We initialize L to the identity matrix, $\boldsymbol{\mu}$ to zero vector and we use the previous initial distribution $q_0(\boldsymbol{\epsilon}_0) = \mathcal{N}(\boldsymbol{\epsilon}_0 | \boldsymbol{\mu}_0, I)$. We then apply Algorithm 1 for 2000 iterations, where we learn $(\boldsymbol{\mu}, L)$, and for different values $t = 0, 5, 20$. The MCMC transition kernel was based on a standard random walk Metropolis-Hastings proposal $\mathcal{N}(\boldsymbol{\epsilon}' | \boldsymbol{\epsilon}, \delta I)$. The first row of Figure 3 shows the untransformed initial samples $\boldsymbol{\epsilon}_0 \sim q_0(\boldsymbol{\epsilon}_0)$ together with the corresponding MCMC samples $\boldsymbol{\epsilon} \sim q_t(\boldsymbol{\epsilon})$. The second row shows the exact samples from the banana-shaped distribution together with the approximate samples $\mathbf{z} = L\boldsymbol{\epsilon} + \boldsymbol{\mu}$, where $\boldsymbol{\epsilon} \sim q_t(\boldsymbol{\epsilon})$. Also the black lines in the second row of Figure 3 visualize the learned transformation parameters $(\boldsymbol{\mu}, L)$ which are displayed as contours of the Gaussian distribution $\mathcal{N}(\boldsymbol{\mu} + \boldsymbol{\mu}_0, LL^T)$. From Figure 3 we can observe the following. Firstly, for $t = 0$ the method reduces to fitting a Gaussian approximation with standard reparametrization-based stochastic VI. Secondly, as t increases the underlying implicit distribution $q_t(\mathbf{z})$ fits better the shape of the distribution. The black contours indicate that the inferred values $(\boldsymbol{\mu}, L)$ depend crucially on t (and the underlying MCMC operation) and they allow to locate the approximation around the highest probability area of the banana-shaped distribution. Notice also that due to the nature of the KL divergence used the approximation tends to be inclusive.

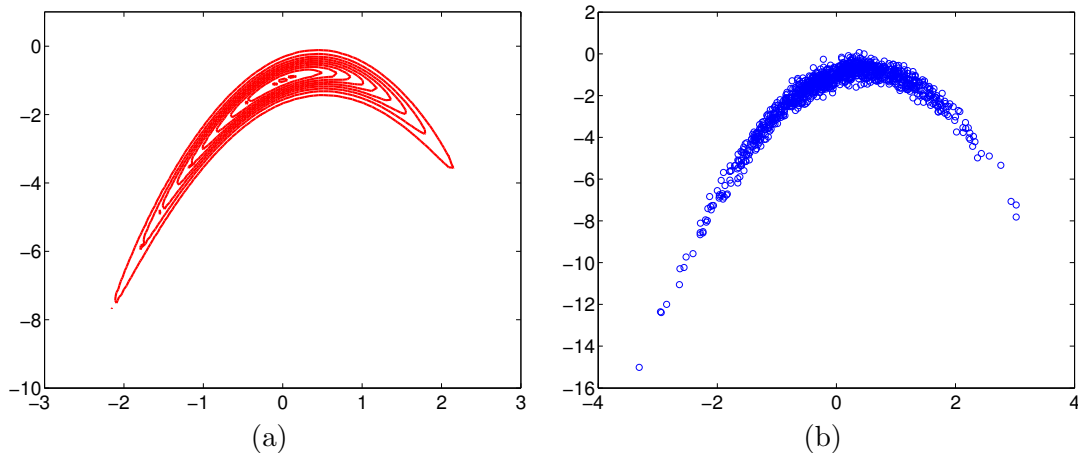


Figure 1: Panel (a) shows contours of the banana-shaped distribution, while panel (b) shows 1000 independent samples.

Finally, we repeated all runs for $t = 0, 5, 20$ by simplifying the affine transformation to a simple translation $\mathbf{z} = \boldsymbol{\epsilon} + \boldsymbol{\mu}$ and by changing the initial distribution to a point delta function $q_0(\boldsymbol{\epsilon}) = \delta(\boldsymbol{\epsilon} - \boldsymbol{\mu}_0)$. Figure 4 shows the exact samples from the banana-shaped distribution together with the approximate samples $\mathbf{z} = \boldsymbol{\epsilon} + \boldsymbol{\mu}$. The black small circle shows the learned translation vector $\boldsymbol{\mu}$ which when $t = 0$, as mentioned in Section 2.2, corresponds to the MAP estimate.

4.2 Variational autoencoders

Here, we consider an application to amortised inference using variational autoencoders (VAEs) [19, 30]. Assume a data set $X = \{\mathbf{x}_1, \dots, \mathbf{x}_n\}$ associated with latent variables $Z = \{\mathbf{z}_1, \dots, \mathbf{z}_n\}$ so that each data point \mathbf{x}_n is generated through a latent variable \mathbf{z}_n . The joint distribution of

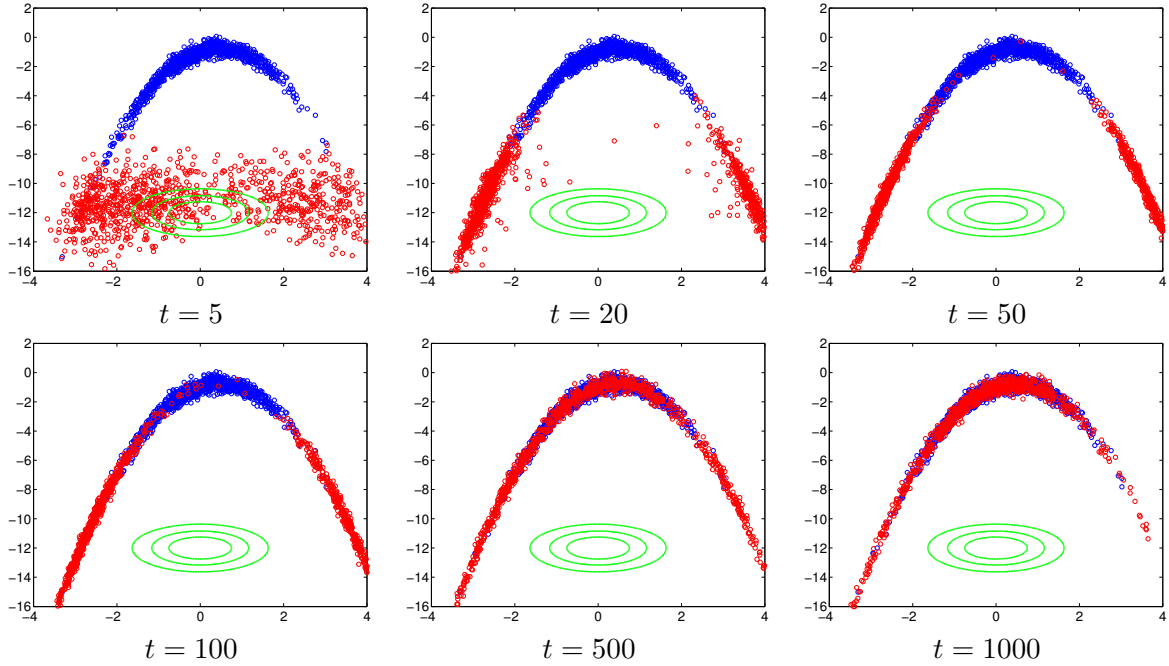


Figure 2: Samples from MCMC marginal distributions (red colour) for different number of iterations. Exact samples are shown with blue colour. Green contours show the initial distribution.

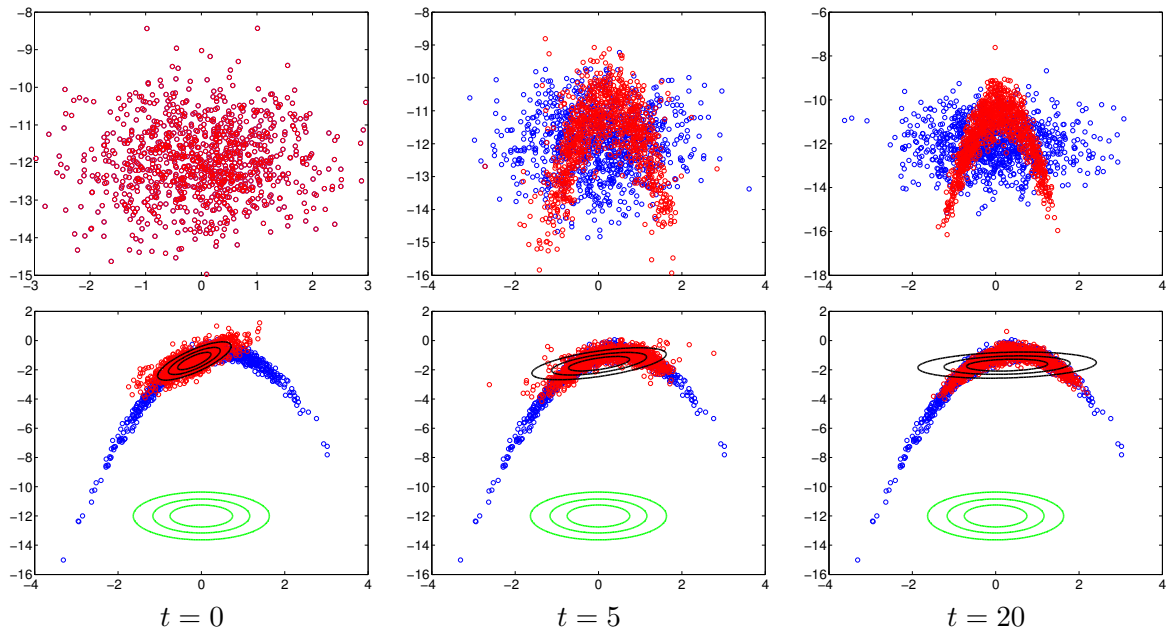


Figure 3: Panels in the first row show the untransformed samples ϵ_0 (blue colour) together with the corresponding MCMC samples $\epsilon \sim q_t(\epsilon)$ (red colour). The second row shows exact samples (blue colour) of the banana-shaped distribution together with the approximate samples $\mathbf{z} = L\epsilon + \mu$ (red colour). Green contours show the initial distribution and black contours visualize the learned transformation parameters (μ, L) .

observations and latent variables is given by

$$p(X, Z) = \prod_{i=1}^m p(\mathbf{x}_i, \mathbf{z}_i; \mathbf{w}). \quad (4)$$

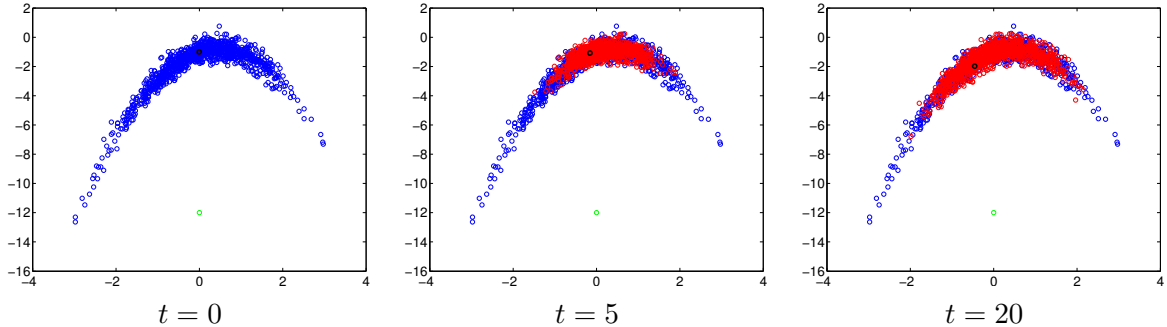


Figure 4: Each panel shows exact samples (blue colour) of the banana-shaped distribution together with the approximate samples $\mathbf{z} = \boldsymbol{\epsilon} + \boldsymbol{\mu}$ (red colour). The green small circles show the initial distribution while the black circles show each learned translation vector $\boldsymbol{\mu}$.

In order to speed up training (when m is large) and also prediction in test data we would like to amortise inference using a recognition model. Based on the framework in Section 2.2 we need to define an invertible transformation for each latent variable \mathbf{z}_i , i.e.

$$\mathbf{z}_i = g(\boldsymbol{\epsilon}_i; \boldsymbol{\theta}(\mathbf{x}_i)), \quad \boldsymbol{\epsilon}_i = g^{-1}(\mathbf{z}_i; \boldsymbol{\theta}(\mathbf{x}_i)),$$

where the vector of reparametrization parameters $\boldsymbol{\theta}(\mathbf{x}_i)$ is further parametrized to be a function of the observation \mathbf{x}_i . Then from the joint in eq. (4) we obtain the reparametrized joint given by

$$p(X, E) = \prod_{i=1}^m p(\mathbf{x}_i, \boldsymbol{\epsilon}_i) = \prod_{i=1}^m p(\mathbf{x}_i, g(\boldsymbol{\epsilon}_i; \boldsymbol{\theta}(\mathbf{x}_i)); \mathbf{w}) J(\boldsymbol{\epsilon}_i; \boldsymbol{\theta}(\mathbf{x}_i)). \quad (5)$$

The overall variational lower bound is obtained by bounding each log likelihood term $\log p(\mathbf{x}_i) = \log \int p(\mathbf{x}_i, \boldsymbol{\epsilon}_i) d\boldsymbol{\epsilon}_i$ using a variational distribution $q_i(\boldsymbol{\epsilon}_i)$ so that

$$\mathcal{F} = \sum_{i=1}^m \int q_i(\boldsymbol{\epsilon}_i) [\log p(\mathbf{x}_i, g(\boldsymbol{\epsilon}_i; \boldsymbol{\theta}(\mathbf{x}_i))) J(\boldsymbol{\epsilon}_i; \boldsymbol{\theta}(\mathbf{x}_i)) - \log q_i(\boldsymbol{\epsilon}_i)] d\boldsymbol{\epsilon}_i. \quad (6)$$

When $q_i(\boldsymbol{\epsilon}_i)$ is chosen to be the standard normal and $\boldsymbol{\theta}(\mathbf{x}_i)$ is an affine transformation of the form

$$\boldsymbol{\theta}(\mathbf{x}_i) = L(\mathbf{x}_i)\boldsymbol{\epsilon}_i + \boldsymbol{\mu}(\mathbf{x}_i),$$

where $L(\mathbf{x}_i)$ is a positive definite diagonal matrix and $\boldsymbol{\mu}(\mathbf{x}_i)$ a real-valued mean vector (typically both parametrized by neural nets), then the maximization of the lower bound in (6) reduces to the standard variational autoencoder training procedure with factorised Gaussian approximations [19, 30]. Next, we compare this standard approach with our proposed MCMC-based variational approximation where we define each $q_i(\boldsymbol{\epsilon}_i)$ to be a t -step MCMC distribution.

We consider the 50000 binarized MNIST digits and construct the latent variable model $p(\mathbf{x}_i, \mathbf{z}_i; \mathbf{w})$ based on a single hidden layer neural net having as input \mathbf{z}_i and sigmoid outputs that model the probabilities of the factorised Bernoulli likelihood $p(\mathbf{x}_i | \mathbf{z}_i; \mathbf{w})$. Each prior $p(\mathbf{z}_i)$ over the latent variables was chosen to be standard normal. This defines a latent variable model for binary data where the essential difference with traditional models, such as binary PCA and factor analysis, is that the mapping from \mathbf{z}_i to \mathbf{x}_i is non-linear and it is parametrized by a neural net. For the hidden layer we use 200 relu units. The diagonal non-negative elements of $L(\mathbf{x}_i)$ and the real-valued vector $\boldsymbol{\mu}(\mathbf{x}_i)$ were also parametrized with separate neural nets each having a single hidden layer with 200 relu units. We compare three VAE training procedures:

i) the standard VAE using Gaussian approximations where each $q_i(\epsilon_i)$ is a standard normal, ii) a variational approximation corresponding to an MCMC marginal distribution obtained by initializing with a standard normal and then running $t = 2$ Hamiltonian Monte Carlo (HMC) iterations with 5 leap-frog steps and ii) and similarly by using a MCMC marginal obtained by initializing with a standard normal and then running $t = 10$ random walk Metropolis-Hastings (MH) steps with a Gaussian proposal distribution. For the parameters \mathbf{w} of the latent variable model we carry out point estimation (see Algorithm 1). All methods were applied using the same learning schedule for 5×10^4 iterations with minibatch size 100 and by using only one sample over ϵ_i when doing parameter updates. The step sizes of HMC and MH were tuned so that to obtain acceptance rates around 90% and 40% respectively. Figure 5 displays the evolution of the stochastic bound without the intractable $-\log q_i(\epsilon)$ term² (i.e. only the log joint term that indicates data reconstruction) for all three methods. Clearly, both MCMC-based methods lead to better training since they allow to express more flexible implicit variational distributions that can fit better the shape of each latent variable posterior. Also the HMC-based marginal works better than the MH-based marginal.

Amortised inference allows to quickly express an variational approximation to some latent variable posterior $p(\mathbf{z}_*|\mathbf{x}_*; \mathbf{w})$, where for instance \mathbf{x}_* could be a test example, without requiring to perform further optimization. For the proposed methods this approximation is implicit, i.e. we first express $\epsilon_* \sim q_*(\epsilon_*)$ by running t MCMC iterations and then an independent sample from the approximate posterior is given by $\mathbf{z}_* = L(\mathbf{x}_*)\epsilon_* + \boldsymbol{\mu}(\mathbf{x}_*)$. Such a sample \mathbf{z}_* can be thought of as a possible latent representation of \mathbf{x}_* that can be used for instance to reconstruct \mathbf{x}_* . Figure 6 shows some test data (first row) together with the corresponding reconstructions obtained by the standard Gaussian approximation (second row) and by the HMC-based variational method (third row). Clearly, the reconstructions based on the proposed method are better. For instance, the right most digit is reconstructed as "9" by the Gaussian approximation while correctly is reconstructed as "4" by the proposed method. Further details and quantitative scores across all 10000 test data are given in the caption of Figure 6.

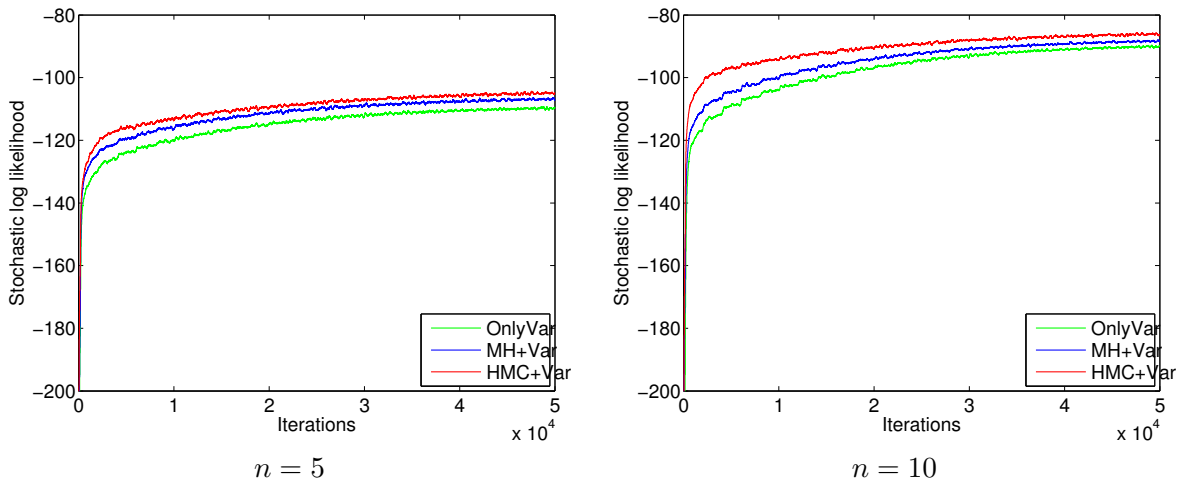


Figure 5: The left panel shows the stochastic bounds (smoothed using a rolling window over 200 actual values) without the $-\log q_i(\mathbf{z}_i)$ term for the three compared methods when the dimensionality of the variable \mathbf{z}_i is $n = 5$, while the right panel shows the same quantities for $n = 10$. The label OnlyVar indicates the standard VAE with a Gaussian approximation, while HMC+Var and MH+Var indicate two proposed schemes that combine MCMC and VI.

²Recall that for the proposed MCMC-based variational method $\log q_i(\epsilon)$ is not tractable since $q_i(\epsilon)$ is implicit.

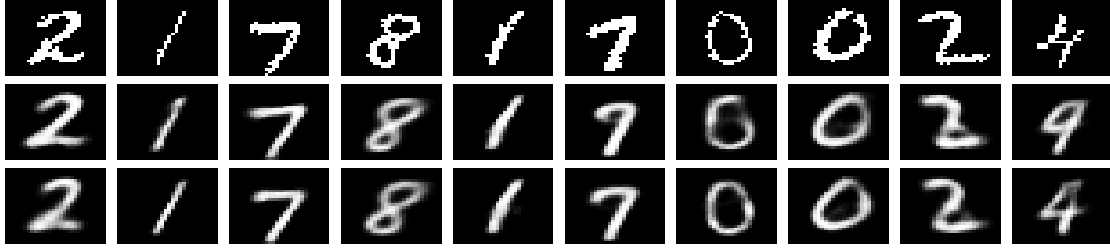


Figure 6: The panels in the first row show some test digits. The panels in the second row show reconstructions obtained by the standard Gaussian approximation (i.e. the OnlyVar method) while the panels in the third row show the reconstructions of the HMC+Var method. These reconstructions were obtained by assuming latent dimensionality $n = 5$. The average reconstructions across all 10000 test examples, measured by cross entropy between each binary digit and its predictive probability vector, was -111.2939 for OnlyVar and -104.1400 for HMC+Var. When $n = 10$ the corresponding numbers were -87.3213 and -82.3134 .

5 Discussion

We have presented an algorithm that combines MCMC and variational inference and it can auto-tune its performance by learning model-based reparametrizations. This is an implicit variational inference algorithm that makes use of the reparametrization trick and fits complex MCMC distributions to exact posteriors without requiring the estimation of log density ratios.

A limitation of the current approach is that it is applicable only to models where we can define a learnable model-based reparametrization (this is typically possible for continuous and differentiable models). For the future it would be interesting to develop alternative and more general ways to combine MCMC and variational inference that would be applicable to arbitrary models such as those that require inference over discrete variables. A preliminary attempt to develop a general procedure based on the score function method, that covers also discrete variables, is described in the Appendix.

References

- [1] C. Andrieu and J. Thoms. A tutorial on adaptive MCMC. *Statistics and Computing*, 18:343–373, 2008.
- [2] Steve Brooks, Andrew Gelman, Galin L . Jones, and Xiao-Li Meng. *Handbook of Markov Chain Monte Carlo (Chapman & Hall/CRC Handbooks of Modern Statistical Methods)*. Chapman and Hall/CRC, 1 edition, May 2011.
- [3] P. Carbonetto, M. King, and F. Hamze. A stochastic approximation method for inference in probabilistic graphical models. In *Advances in Neural Information Processing Systems*, 2009.
- [4] Bob Carpenter, Andrew Gelman, Matthew Hoffman, Daniel Lee, Ben Goodrich, Michael Betancourt, Marcus Brubaker, Jiqiang Guo, Peter Li, and Allen Riddell. Stan: A probabilistic programming language. *Journal of Statistical Software*, 76(1), 2017.
- [5] Edward Challis and David Barber. Concave gaussian variational approximations for inference in large-scale bayesian linear models. In *AISTATS*, pages 199–207, 2011.
- [6] Thomas M. Cover and Joy A. Thomas. *Elements of Information Theory*. Wiley-Interscience, New York, NY, USA, 1991.
- [7] Justin Domke. A divergence bound for hybrids of MCMC and variational inference and an application to langevin dynamics and SGVI. In *Proceedings of the 34th International Conference on Machine Learning, ICML 2017, Sydney, NSW, Australia, 6-11 August 2017*, pages 1029–1038, 2017.

- [8] S. Duane, A. D. Kennedy, B. J. Pendleton, and D. Roweth. Hybrid Monte Carlo. *Physics Letters B*, 195(2):216–222, 1987.
- [9] Mark Girolami and Ben Calderhead. Riemann manifold Langevin and Hamiltonian Monte Carlo methods. *Journal of the Royal Statistical Society: Series B (Statistical Methodology)*, 73(2):123–214, 2011.
- [10] P. W. Glynn. Likelihood ratio gradient estimation for stochastic systems. *Communications of the ACM*, 33(10):75–84, oct 1990.
- [11] Ian Goodfellow, Jean Pouget-Abadie, Mehdi Mirza, Bing Xu, David Warde-Farley, Sherjil Ozair, Aaron Courville, and Yoshua Bengio. Generative adversarial nets. In Z. Ghahramani, M. Welling, C. Cortes, N. D. Lawrence, and K. Q. Weinberger, editors, *Advances in Neural Information Processing Systems 27*, pages 2672–2680. Curran Associates, Inc., 2014.
- [12] H. Haario, E. Saksman, and J. Tamminen. An adaptive metropolis algorithm. *Bernoulli*, 7:223–240, 2001.
- [13] Matthew D. Hoffman, David M. Blei, and Francis R. Bach. Online learning for latent dirichlet allocation. In *NIPS*, pages 856–864, 2010.
- [14] Matthew D. Hoffman, David M. Blei, Chong Wang, and John William Paisley. Stochastic variational inference. *Journal of Machine Learning Research*, 14(1):1303–1347, 2013.
- [15] Matthew D. Hoffman and Andrew Gelman. The no-u-turn sampler: Adaptively setting path lengths in hamiltonian monte carlo. *J. Mach. Learn. Res.*, 15(1):1593–1623, January 2014.
- [16] Ferenc Huszar. Variational inference using implicit distributions. *CoRR*, abs/1702.08235, 2017.
- [17] Michael I. Jordan, Zoubin Ghahramani, Tommi S. Jaakkola, and Lawrence K. Saul. An introduction to variational methods for graphical models. *Mach. Learn.*, 37(2):183–233, November 1999.
- [18] Theofanis Karaletsos. Adversarial message passing for graphical models. *CoRR*, abs/1612.05048, 2016.
- [19] D. P. Kingma and M. Welling. Auto-encoding variational Bayes. In *International Conference on Learning Representations*, 2014.
- [20] A. Kucukelbir, D. Tran, R. Ranganath, A. Gelman, and D. M. Blei. Automatic differentiation variational inference. *arXiv:1603.00788*, 2016.
- [21] Yingzhen Li, Richard E. Turner, and Qiang Liu. Approximate inference with amortised MCMC. *CoRR*, abs/1702.08343, 2017.
- [22] Qiang Liu and Dilin Wang. Stein variational gradient descent: A general purpose bayesian inference algorithm. In D. D. Lee, M. Sugiyama, U. V. Luxburg, I. Guyon, and R. Garnett, editors, *Advances in Neural Information Processing Systems 29*, pages 2378–2386. 2016.
- [23] Lars M. Mescheder, Sebastian Nowozin, and Andreas Geiger. Adversarial variational bayes: Unifying variational autoencoders and generative adversarial networks. In *Proceedings of the 34th International Conference on Machine Learning, ICML 2017, Sydney, NSW, Australia, 6-11 August 2017*, pages 2391–2400, 2017.
- [24] A. Mnih and K. Gregor. Neural variational inference and learning in belief networks. In *International Conference on Machine Learning*, 2014.
- [25] Radford M. Neal. MCMC using Hamiltonian dynamics. *Handbook of Markov Chain Monte Carlo*, 54:113–162, 2010.
- [26] J. W. Paisley, D. M. Blei, and M. I. Jordan. Variational Bayesian inference with stochastic search. In *International Conference on Machine Learning*, 2012.
- [27] Omiros Papaspiliopoulos, Gareth O. Roberts, and Martin Sköld. Non-centered parameterizations for hierarchical models and data augmentation. In *Bayesian statistics, 7 (Tenerife, 2002)*, pages 307–326. Oxford Univ. Press, New York, 2003. With a discussion by Alan E. Gelfand, Ole F. Christensen and Darren J. Wilkinson, and a reply by the authors.

- [28] R. Ranganath, S. Gerrish, and D. M. Blei. Black box variational inference. In *Artificial Intelligence and Statistics*, 2014.
- [29] Rajesh Ranganath, Dustin Tran, Jaan Altosaar, and David Blei. Operator variational inference. In D. D. Lee, M. Sugiyama, U. V. Luxburg, I. Guyon, and R. Garnett, editors, *Advances in Neural Information Processing Systems 29*, pages 496–504. 2016.
- [30] D. J. Rezende, S. Mohamed, and D. Wierstra. Stochastic backpropagation and approximate inference in deep generative models. In *International Conference on Machine Learning*, 2014.
- [31] Danilo Jimenez Rezende and Shakir Mohamed. Variational inference with normalizing flows. In *Proceedings of the 32nd International Conference on Machine Learning, ICML 2015, Lille, France, 6-11 July 2015*, pages 1530–1538, 2015.
- [32] Herbert Robbins and Sutton Monro. A Stochastic Approximation Method. *The Annals of Mathematical Statistics*, 22(3):400–407, 1951.
- [33] Christian P. Robert and George Casella. *Monte Carlo Statistical Methods (Springer Texts in Statistics)*. Springer-Verlag New York, Inc., Secaucus, NJ, USA, 2005.
- [34] F. J. R. Ruiz, M. K. Titsias, and D. M. Blei. Overdispersed black-box variational inference. In *Uncertainty in Artificial Intelligence*, 2016.
- [35] T. Salimans and D. A. Knowles. Fixed-form variational posterior approximation through stochastic linear regression. *Bayesian Analysis*, 8(4):837–882, 2013.
- [36] Tim Salimans, Diederik Kingma, and Max Welling. Markov chain monte carlo and variational inference: Bridging the gap. In *Proceedings of the 32nd International Conference on Machine Learning, ICML 2015, Lille, France, 6-11 July 2015*, pages 1530–1538. JMLR Workshop and Conference Proceedings, 2015.
- [37] Masashi Sugiyama, Taiji Suzuki, and Takafumi Kanamori. *Density Ratio Estimation in Machine Learning*. Cambridge University Press, New York, NY, USA, 1st edition, 2012.
- [38] M. K. Titsias and M. Lázaro-Gredilla. Doubly stochastic variational Bayes for non-conjugate inference. In *International Conference on Machine Learning*, 2014.
- [39] Dustin Tran, Rajesh Ranganath, and David M. Blei. Deep and hierarchical implicit models. *CoRR*, abs/1702.08896, 2017.
- [40] Martin J. Wainwright and Michael I. Jordan. Graphical models, exponential families, and variational inference. *Found. Trends Mach. Learn.*, 1(1-2):1–305, January 2008.
- [41] D. Wang and Q. Liu. Learning to draw samples: With application to amortized mle for generative adversarial learning. *CoRR*, abs/1611.01722, 2017.
- [42] Greg C. G. Wei and Martin A. Tanner. A Monte Carlo Implementation of the EM Algorithm and the Poor Man’s Data Augmentation Algorithms. *Journal of the American Statistical Association*, 85(411):699–704, 1990.
- [43] Max Welling and Yee Whye Teh. Bayesian learning via stochastic gradient langevin dynamics. In Lise Getoor and Tobias Scheffer, editors, *ICML*, pages 681–688. Omnipress, 2011.
- [44] R. J. Williams. Simple statistical gradient-following algorithms for connectionist reinforcement learning. *Machine Learning*, 8(3–4):229–256, 1992.

A MCMC-based implicit variational inference using the score function method

The term explicit distribution refers to a distribution such that we can both simulate from and tractably evaluate its density, while the term implicit distribution refers to a distribution from which we can only sample. Next the Dirac delta mass $\delta(\mathbf{z})$ would be considered as an explicit

distribution. A general way to construct implicit distributions is by using the following mixture representation

$$q(\mathbf{z}) = \int Q(\mathbf{z}|\mathbf{z}_0)q(\mathbf{z}_0)d\mathbf{z}_0,$$

where \mathbf{z}_0 does not have to live in the same space as \mathbf{z} . The simplest choice of having an implicit $q(\mathbf{z})$ is to assume that both $q(\mathbf{z}_0)$ and $Q(\mathbf{z}|\mathbf{z}_0)$ are explicit but the integral is intractable. An example of this, very popular in recent complex generative models based on adversarial training [11], is to set $q(\mathbf{z}_0)$ to be a simple Gaussian or uniform, and define $Q(\mathbf{z}|\mathbf{z}_0)$ from a neural net mapping $\mathbf{z} = f(\mathbf{z}_0; \boldsymbol{\theta})$ having as input the vector \mathbf{z}_0 and parameters $\boldsymbol{\theta}$. The latter essentially sets $Q(\mathbf{z}|\mathbf{z}_0)$ equal to the Dirac delta function $\delta(\mathbf{z} - f(\mathbf{z}_0; \boldsymbol{\theta}))$. Other ways to obtain an implicit $q(\mathbf{z})$ is by allowing $q(\mathbf{z}_0)$ and/or $Q(\mathbf{z}|\mathbf{z}_0)$ to be also implicit. The MCMC-based variational inference method that we presented in the main paper belongs to this latter category where $q(\mathbf{z}_0) \equiv q_t(\boldsymbol{\epsilon})$ is an implicit MCMC marginal, $Q(\mathbf{z}|\mathbf{z}_0) \equiv \delta(\mathbf{z} - g(\boldsymbol{\epsilon}; \boldsymbol{\theta}))$ and $\mathbf{z}_0 \equiv \boldsymbol{\epsilon}$. The ability to reparametrize the variational lower bound was due to the invertibility of $g(\boldsymbol{\epsilon}; \boldsymbol{\theta})$. Next we will discuss a different combination of MCMC and variational inference by setting $q(\mathbf{z}_0)$ to a simple explicit distribution and constructing $Q(\mathbf{z}|\mathbf{z}_0)$ based on MCMC.

Suppose a MCMC marginal distribution $q_t(\mathbf{z})$ with transition kernel $q(\mathbf{z}'|\mathbf{z})$ that targets the posterior of interest $p(\mathbf{z}|\mathbf{x})$. Specifically, $q_t(\mathbf{z})$ is constructed by an initial distribution $q_0(\mathbf{z}_0; \boldsymbol{\theta})$, that depends on tunable parameters $\boldsymbol{\theta}$, and the compound transition density $Q_t(\mathbf{z}|\mathbf{z}_0)$ corresponding to t MCMC iterations, i.e.

$$q_t(\mathbf{z}) = \int Q_t(\mathbf{z}|\mathbf{z}_0)q_0(\mathbf{z}_0; \boldsymbol{\theta})d\mathbf{z}_0. \quad (7)$$

Notice that $Q_t(\mathbf{z}|\mathbf{z}_0)$ is implicit while $q_0(\mathbf{z}_0; \boldsymbol{\theta})$ is explicit. We wish to use $q_t(\mathbf{z})$ as a variational distribution and optimize it over the parameters $\boldsymbol{\theta}$ that determine the explicit component $q_0(\mathbf{z}_0; \boldsymbol{\theta})$. Since $q_0(\mathbf{z}_0; \boldsymbol{\theta})$ determines the initialization of MCMC, by tuning $\boldsymbol{\theta}$ we are essentially learning how to start in order to speed up MCMC convergence within the budget of t iterations. The minimization of $\text{KL}(q_t(\mathbf{z})||p(\mathbf{z}|\mathbf{x}))$ leads to the maximization of the lower bound

$$\mathcal{F}_t(\boldsymbol{\theta}) = \mathbb{E}_{q_t(\mathbf{z})}[\log p(\mathbf{x}, \mathbf{z}) - \log q_t(\mathbf{z})].$$

By taking gradients with respect to $\boldsymbol{\theta}$ and by making use of the identity $\int q_t(\mathbf{z})\nabla_{\boldsymbol{\theta}} \log q_t(\mathbf{z})d\mathbf{z} = 0$ we have

$$\begin{aligned} \nabla_{\boldsymbol{\theta}}\mathcal{F}_t(\boldsymbol{\theta}) &= \int_{\mathbf{z}} \nabla_{\boldsymbol{\theta}}q_t(\mathbf{z}) [\log p(\mathbf{x}, \mathbf{z}) - \log q_t(\mathbf{z})] d\mathbf{z} \\ &= \int_{\mathbf{z}} \left(\int_{\mathbf{z}_0} Q_t(\mathbf{z}|\mathbf{z}_0)\nabla_{\boldsymbol{\theta}}q_0(\mathbf{z}_0; \boldsymbol{\theta})d\mathbf{z}_0 \right) [\log p(\mathbf{x}, \mathbf{z}) - \log q_t(\mathbf{z})] d\mathbf{z} \\ &= \int_{\mathbf{z}} Q_t(\mathbf{z}|\mathbf{z}_0) \left(\int_{\mathbf{z}_0} q_0(\mathbf{z}_0; \boldsymbol{\theta})\nabla_{\boldsymbol{\theta}} \log q_0(\mathbf{z}_0; \boldsymbol{\theta})d\mathbf{z}_0 \right) [\log p(\mathbf{x}, \mathbf{z}) - \log q_t(\mathbf{z})] d\mathbf{z}, \end{aligned}$$

where in the second line we used (7) and in third one the score function method, also called log-derivative trick or REINFORCE [44, 10]. An unbiased estimate of the gradient can be obtained by drawing a set of samples $\{\mathbf{z}_0^{(s)}, \mathbf{z}^{(s)}\}_{s=1}^S$ where each $\mathbf{z}_0^{(s)} \sim q_0(\mathbf{z}_0; \boldsymbol{\theta})$ and $\mathbf{z}^{(s)} \sim Q_t(\mathbf{z}|\mathbf{z}_0^{(s)})$, i.e. $\mathbf{z}^{(s)}$ is the final state of an MCMC run of length t when starting from $\mathbf{z}_0^{(s)}$, and then using

$$\frac{1}{S} \sum_{s=1}^S \nabla_{\boldsymbol{\theta}} \log q_0(\mathbf{z}_0^{(s)}; \boldsymbol{\theta}) \left[\log p(\mathbf{x}, \mathbf{z}^{(s)}) - \log q_t(\mathbf{z}^{(s)}) \right]. \quad (8)$$

This estimate is still intractable because $q_t(\mathbf{z})$ is implicit and we cannot evaluate the term $\log q_t(\mathbf{z})$. A way to get around this problem is to approximate $\log q_t(\mathbf{z})$ by applying log density

ratio estimation. However, this can be very difficult in high-dimensional settings and therefore the ability to get reliable estimates for $\log q_t(\mathbf{z})$ is the main obstacle for the general applicability of the above framework.